frontiers | Frontiers in Earth Science

TYPE Original Research
PUBLISHED 22 January 2024
DOI 10.3389/feart.2024.1334074

OPEN ACCESS

EDITED BY
Haijun Qiu,
Northwest University, China

REVIEWED BY
Mingtao Ding,
Southwest Jiaotong University, China
Zheng Han,
Central South University, China

*CORRESPONDENCE
Zhiquan Yang,
yzq1983816@kust.edu.cn

RECEIVED 09 November 2023
ACCEPTED 08 January 2024
PUBLISHED 22 January 2024

CITATION
Shen H, Yang Z, Hu G, Tian S, Rahman M, Ren J and Zhang Y (2024), Causal mechanisms and evolution processes of "block-burst" debris flow hazard chains in mountainous urban areas: a case study of Meilong gully in Danba county, Sichuan Province, China.
Front. Earth Sci. 12:1334074.
doi: 10.3389/feart.2024.1334074

Causal mechanisms and evolution processes of "block-burst" debris flow hazard chains in mountainous urban areas: a case study of Meilong gully in Danba county, Sichuan Province, China

Haowen Shen[1,2,3], Zhiquan Yang[1,3,4]*, Guisheng Hu[2,5], Shufeng Tian[2], Mahfuzur Rahman[6], Jincheng Ren[1,3,4] and Yong Zhang[7]

[1]Faculty of Public Safety and Emergency Management, Kunming University of Science and Technology, Kunming, China, [2]Key Lab of Mountain Hazards and Surface Processes, Institute of Mountain Hazards and Environment, Chinese Academy of Sciences, Chengdu, China, [3]Key Laboratory of Geological Disaster Risk Prevention and Control and Emergency Disaster Reduction of Ministry of Emergency Management of the People's Republic of China, Kunming, China, [4]Key Laboratory of Early Rapid Identification, Prevention and Control of Geological Diseases in Traffic Corridor of High Intensity Earthquake Mountainous Area of Yunnan Province, Kunming, China, [5]Academy of Plateau Science and Sustainability, Xining, China, [6]Department of Civil Engineering, International University of Business Agriculture and Technology (IUBAT), Dhaka, Bangladesh, [7]Anyang Institute of Technology, Anyang, China

The research interest in multi-hazard chains lies in the comprehension of how various hazards, such as debris flows, floods, and landslides, can interact and amplify one another, resulting in cascading or interconnected hazards. On 17 June 2020, at approximately 3:20 a.m., a debris flow occurred in Meilong gully (MLG), located in Banshanmen Town, Danba County, in southwest China's Sichuan Province. The debris flow had a discharge volume of approximately 40 × 10^4 m^3 and rushed out to block the Xiaojinchuan (XJC) river, subsequently forming a barrier lake. This event ultimately induced a hazard chain that included heavy rainfall, debris flow, landslides, the formation of a barrier lake, and an outburst flood. The impact of this chain resulted in the displacement of 48 households and affected 175 individuals. Furthermore, it led to the destruction of an 18 km section of National Highway G350, stretching from Xiaojin to Danba County, causing economic losses estimated at 65 million yuan. The objective of this study is to analyze the factors leading to the formation of this hazard chain, elucidate its triggering mechanisms, and provide insights for urban areas in the western mountainous region of Sichuan to prevent similar dam-break type debris flow hazard chains. The research findings, derived from field investigations, remote sensing imagery analysis, and parameter calculations, indicate that prior seismic disturbances and multiple dry-wet cycle events increased the volume of loose solid materials within the MLG watershed. Subsequently, heavy rainfall triggered the initiation of the debris flow in MLG. The cascading dam-break, resulting from three unstable slopes and boulders within the channel, amplified the scale of the hazard chain, leading to a

significant amount of solid material rushing into the XJC river, thus creating a dam that constricted the river channel. With the intensification of river scouring, the reactivation and destabilization of the Aniangzhai (ANZ) paleolandslide occurred, ultimately leading to the breach of the dam and the formation of an outburst flood. The research comprehensively and profoundly reveals the causal mechanism of the MLG hazard chain, and proposes measures to disrupt the chain at various stages, which can aid in enhancing monitoring, early warning, forecasting systems, and identifying key directions for ecological environmental protection in urban areas within the western mountainous region of Sichuan. Additionally, it could also serve as a reference for mountainous urban areas such as the Tianshan, Alps, Rocky Mountains, and Andes, among others.

KEYWORDS

debris flow, hazard chain, slope instability, formation and evolution mechanism, monitoring and early warning, risk assessment

1 Introduction

The study of hazard chains has gained significant attention in recent years, particularly in the context of large-scale debris flow hazards in high mountain and canyon areas. These hazards often trigger a series of interconnected events, including landslides, barrier lakes, and outburst floods. Examples of such hazard chains can be found in various regions, including the Qinghai-Tibet Plateau (CUI et al., 2015; Liu et al., 2023b), the western Sichuan Plateau (Chen et al., 2011), the Italian Alps (Deganutti et al., 2000), the island of Elba (Iotti and Simoni, 1997), Taiwan (Cheng et al., 2000), the SE coast of Australia (Flentje et al., 2000), and Nicaragua (Scott, 2000).

The combination and overlapping impact of multiple hazards create a secondary hazard chain that poses a significantly greater threat than the direct impact of a single debris flow. This phenomenon underscores the complex and interconnected nature of natural disasters, highlighting the need for comprehensive understanding and effective mitigation strategies (Guo et al., 2021; Guo et al., 2022). Mountain hazard chain causes enormous damage to transportation routes, agricultural and forestry economy, ecological environment and the safety of urban residents. For example, in 2018, the Baige landslide in Tibet led to the formation of a dam that blocked the Jinsha River, resulting in severe downstream flooding and devastating economic losses (Zhang et al., 2019; Zhang et al., 2020a; Zhong et al., 2020). Similarly, on 17 October 2018, at approximately 5 a.m., an ice and rock avalanche in Tibet triggered a debris flow, leading to the formation of a barrier lake that posed a significant threat to the lives and property of residents in upstream and downstream towns, as well as the ecological environment and transportation networks in the vicinity (Hu et al., 2019; Liu et al., 2023b; Yang et al., 2023b; Yang et al., 2023d). The devastating impact of hazard chains was exemplified by the extensive floods, landslides, and debris flows that occurred in Venezuela on December 15–16, 1999, causing the worst natural disaster in the country's history, resulting in significant loss of life and widespread destruction of homes and structures. This historical event serves as a poignant reminder of the far-reaching consequences of interconnected hazards and the importance of understanding and mitigating the secondary disaster chain effects (Pérez, 2001).

In the context of studying hazard chains, the Meilong gully (MLG) hazard chain in Danba County, Sichuan Province, China, occurred on 17 June 2020, has emerged as a rare and valuable case for analysis, shedding light on the complexities and implications of such interconnected hazards. The MLG hazard chain in Danba County was triggered by heavy rainfall. However, during the same period, in Zengda gully, Dajin County, Sichuan Province, China, which is located less than 1.2 km away and has a larger watershed area of 125.53 km^2, no debris flow occurred. According to the literature, Zengda gully has experienced six debris flow hazards since the 1990s, with the latest one occurred on 27 June 2019 (Hu et al., 2022). Despite the similarities in topography, geomorphology, and climatic conditions, Zengda gully, with a larger drainage area and more sediment sources, did not experience a debris flow event.

Currently, scholars have conducted research in the MLG watershed. A simulation was conducted to analyze the movement and accumulation process of MLG debris flow (An et al., 2022). Additionally, Ning et al. (2022) analyzedthe implementation of engineering measures aimed at slowing down and reducing the ongoing development of the MLG hazard chain. Liu et al. (2023a) conducted numerical simulations of the XJC river dam failure process and identified that the channel uplift resulting from the dam failure exacerbated the flood hazard of the MLG hazard chain. However, these studies have not revealed the entire process and mechanism of the formation, development, evolution, and hazard-causing of the MLG debris flow hazard chain under the internal and external dynamic coupling. Unlike the simple superposition of single or multiple hazards, the mountain hazard chains often have temporal and spatial continuity and extension, and exhibit cascading and compound effects, often characterized by huge damage, wide impact range, and long duration (Chen and Cui, 2017; Mani et al., 2023). With the acceleration of economic development and population growth, engineering activities in mountainous urban areas in western Sichuan are also increasing rapidly (Wang et al., 2018). At the same time, slope instability, debris flows, and other mountain hazards and their secondary hazard chains are also threatening the safety of mountainous urban areas.

In this context, using the MLG hazard chain that occurred in Danba County, Sichuan Province, China, as a case study, this research investigates the triggering mechanism of debris flow

under the combined influence of earthquakes and multiple dry-wet cycles, in addition to the heavy rainfall factor. This article is pioneering in its utilization of the dry-wet cycle within long-term rainfall sequences to analyze the promotion effect of increased loose source materials on the formation of debris flow in the MLG watershed. It elucidates the whole process of the MLG hazard chain, encompassing formation, occurrence, scale amplification, and disaster. Furthermore, it examined the mechanisms leading to the formation of secondary hazards within the chain. The results shed light on the factors behind the tendency of "block-burst" type debris flow hazard chains in mountainous urban areas in western Sichuan to be large in scale and result in substantial losses. These findings also serve as a reminder that, in future mountainous urban development, it is imperative to accurately identify debris flow gullies and to take into account the impacts of pre-earthquakes, dry-wet cycles, and channel blockages during geological hazard risk assessments.

2 Materials and methods

2.1 Background

2.1.1 Geographic and geomorphic background of the study area

MLG is situated in the high mountain canyon region of western Sichuan Province, specifically in Guanzhou Village, Banshanmen Town, Danba County, within the Ganzi Tibetan Autonomous Prefecture (see Figure 1). Access to MLG is available via the G350 national highway leading to the gully entrance. The geographic coordinates of the MLG debris flow gully entrance are as follows: N30°59′25.11″, E102°1′32.20". The drainage area of MLG spans 62.79 km^2, with the main ditch extending over a length of 12.42 km. The highest point within the watershed reaches an elevation of 4,760 m, while the lowest point is located at the entrance of the XJC river at an elevation of 2,120 m, resulting in a relative height difference of 2,640 m. The average longitudinal drop across the watershed is approximately 212.56 per mille, with the accumulation area near the gully mouth featuring a gentler slope, averaging around 100 per mille. The MLG watershed encompasses ten branch ditches, and the extent of the watershed and its topographic characteristics are illustrated in Figure 1.

2.1.2 Topographic features and earthquakes

The study area is situated within a triangular fault block, enclosed by the Freshwater River Fault, the Longmenshan Fault, and the South Qinling Fault Zone. This region is characterized by high tectonic activity and the presence of well-developed faults. The exposed geological strata in the MLG watershed predominantly consist of clastic rocks from the Devonian Guiguan Group (Dwg), as well as Quaternary avalanche deposits and alluvial soils (refer to Figure 1). Notably, this study area has experienced frequent seismic events in recent history, including significant earthquakes such as the 7.9 magnitude quake in Fuhuo (1973), a 5.0 magnitude event in Tagong (1978), a 6.9 magnitude earthquake in Daofu (1981), an 8.0 magnitude earthquake in Wenchuan (2008), and a 6.3 magnitude earthquake in Kangding (2014), all within the same vicinity (see Figure 1). The most powerful earthquake recorded in this region was the magnitude 8.0 mega-earthquake that struck Yingxiu Township, Wenchuan County, on 12 May 2008.

2.1.3 Meteorological and hydrological characteristics

The study area experiences relatively low average annual rainfall, with a long-term average of 649.34 mm and a maximum annual precipitation of 823.3 mm recorded in 2012. Rainfall is primarily concentrated between May and September, accounting for 82.3% of the annual total, with an average monthly rainfall of about 101 mm during this period, with June having the highest monthly average at 100.5 mm. The average annual temperature is 14.6°C, with the coldest month, January, ranging between 3°C–6°C, and the hottest month, August, typically ranging from 20°C–23°C. The highest recorded temperature in recent years was 39.5°C.

2.2 Methodology

2.2.1 Calculation of debris flow dynamic parameters

The key dynamic parameters for assessing the nature and magnitude of debris flow include density, velocity, and discharge. In this study, field investigations (Figure 2) were conducted, involving the selection of 12 groups for on-site slurry preparation of debris flow samples and the examination of 6 representative sections within the MLG area (Rahman and Konagai, 2017). The parameters characterizing the behavior of debris flow in MLG were determined through a combination of field investigations and laboratory tests. The relevant calculation formulas are as follows (Table 1).

2.2.2 Seismic impact analysis

It has shown that earthquakes can cause landslides and subsequent hazard chains (Fan et al., 2018; Wang et al., 2019). The study combined empirical relationships between earthquakes and landslides, drawing from data provided by the United States Geological Survey seismic database. A total of 720 seismic events with magnitudes exceeding 4, occurring within a 420 km radius centered on MLG, were extracted from the Chinese National Earthquake Science Data Center (http://data.earthquake.cn) and the global seismic database (https://www.usgs.gov/) published by the United States Geological Survey (Keefer, 1984). These data sets were then employed to examine the impact of historical seismic events on the stability of soil formations within the study area.

2.2.3 Drought analysis

The SPI can accomplish the simultaneous assessment of drought because the observed precipitation during each time period is considered a statistical sample from a larger parent population. For computational accuracy, Guttman (1999) recommends a minimum of 50 years of precipitation data. Observational data need not be preprocessed into the desired aggregations; available software codes (such as available from the National Drought Mitigation Center) accept monthly input data [which is usually the minimum

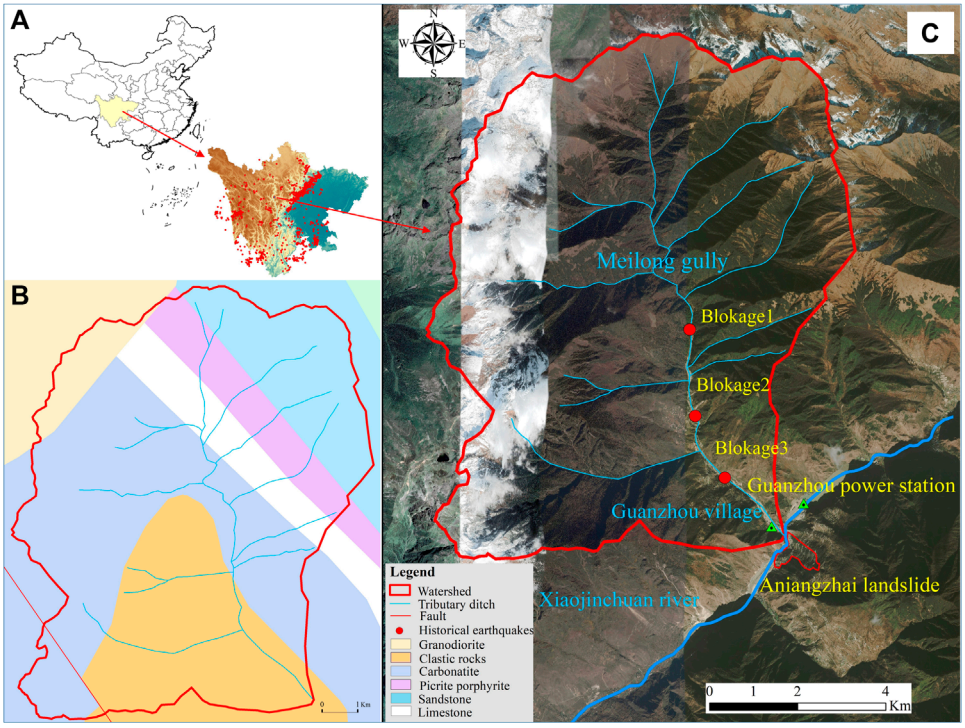

FIGURE 1
Regional setting of the study area. **(A)** The study area is located at the high mountain canyon area of western Sichuan Province and Historical earthquakes with a magnitude greater than 4.0 since 1970 within 420 km centered on MLG. **(B)** Geological background. **(C)** High-resolution remote sensing images of the MLG.

FIGURE 2
On-site soil sampling.

interval frequency used to study drought (i.e., the 1-month SPI)] and aggregate it to desired intervals. Precipitation is known to follow an asymmetric frequency distribution, with the bulk of the occurrences at low values, and a rapidly decreasing likelihood of larger precipitation totals. There are a number of such positively-skewed analytical distributions, six of which were analyzed for SPI computations by Guttman (1999). The distribution for the SPI adopted by McKee et al. (1995), as well as the NDMC, is the incomplete gamma distribution. We first collected historical rainfall data from 1950 to 2020 and then utilized the SPI algorithm in MATLAB to analyze the input data, ultimately obtaining 1-month SPI value.

The 1-month Standardized Precipitation Index (SPI) was employed in this study to evaluate the area's drought and humidity before the disaster (Seiler et al., 2002). The SPI categorizes drought into seven grades based on the values: SPI ≥2 for extremely wet, 1.5 < SPI ≤1.99 for severely wet, 1.0 < SPI ≤1.49 for moderately wet, −0.99 < SPI ≤0.99 for near normal, −1.49 < SPI ≤ −1.0 for moderately dry, −1.99 < SPI ≤ −1.5 for severely dry, and SPI ≤ −2 for extremely dry (McKee et al., 1995). Data were

TABLE 1 Formula tables for debris flow dynamic parameters.

Parameter	Formula	Parameters in the formula
Density	$\gamma_c = G/V$	γ_c is the debris flow density; G is the soil sample weight; V is the soil sample volume
Velocity	$V_c = (M_c/a)H_c^{2/3}I_c^{1/2}$	V_c ais the velocities of the debris flow; I_c is the hydraulic gradient of the debris flow section of the gully obtained by on-site measurement; M_c are the roughness coefficients for debris flows; H_c is the hydraulic radius (m) defined as the mud depth of the debris flow section obtained by on-site measurement. a is the drag coefficient; φ is the increase coefficient; γ_w is the density of water (kg/m^3) determined as 1,000 kg/m^3; γ_s is the density of the solid material (kg/m^3) determined as 2,650 kg/m^3.
	$a = (1+\varphi\gamma_s)^{1/2}$	
	$\varphi = (\gamma_c - \gamma_w)/(\gamma_s - \gamma_c)$	
Discharge	$Q_C = A_{SC} \times V_C$	Q_C is the peak discharge of debris flow (m^3/s), where A_{sc} denotes the area of the cross-section (m^2), and V_C is the average velocity at the cross-section (m/s).

obtained from the National Meteorological Data Center of China (http://data.cma.cn/).

3 Characteristics of MLG hazard chain

3.1 Overview of MLG hazard chain

Based on on-site investigations and related information, MLG experienced a minor mudslide during the flood season of 1952, but it was of a relatively small scale and resulted in no casualties. However, on 17 June 2020, around 3:20 a.m., MLG witnessed a large-scale, infrequent catastrophic mudslide with a recurrence period estimated to be approximately one event in 70 years. This event had significant consequences, including the destruction of an 18 km stretch of National Highway G350 from Xiaojin to Danba (Figures 3A, B). Numerous houses in Guanzhou Village were flooded, resulting in the unfortunate loss of two lives in the area, and it affected 175 villagers from 48 households (as depicted in Figure 3C). Additionally, the substantial material carried by the mudslide in MLG directly obstructed the XJC River, leading to the formation of a barrier lake (Figure 3D). The constriction of the river increased its scouring capacity, destabilizing the ANZ paleolandslide (Figure 3E), and the barrier lake eventually breached, causing an outburst flood that inundated upstream properties and farmland. Simultaneously, this event affected the water discharge of the Guanzhou hydroelectric power station, resulting in a total economic loss estimated at 85 million yuan.

3.2 Calculation results of debris flow motion parameters

3.2.1 Density

As historical monitoring data for debris flow in MLG were lacking, determining the density of the debris flow relied on two methods: on-site preparation of debris flow samples and a table checking method. The weights of the debris flow samples were measured during field investigations, with reference to contemporary debris flows. A total of 12 sets of field experiments were conducted across the upper, middle, and lower reaches of the watershed, as well as in the accumulation area. Additionally, insights from villagers who had witnessed the debris flow events were considered for comparison. This collective data contributed to the calculation of bulk weight parameters for the 12 groups of debris flow samples (as outlined in Table 2). The results revealed an average bulk density of 1.769 g/cm^3 for the MLG debris flow, signifying it as a viscous debris flow.

3.2.2 Velocity and discharge

Discharge serves as a direct indicator of debris flow size and is a pivotal design parameter for prevention and control projects. Calculating debris flow velocity is essential for determining debris flow discharge, which is typically accomplished through morphology investigation methods. Detailed velocity and discharge calculations for six sections within the MLG debris flow are provided in Table 3. The findings reveal that at the mouth of MLG, the debris flow velocity is 4.78 m/s, and the debris flow discharge is 860.40 m^3/s. These results unequivocally classify the MLG debris flow as a large-scale debris flow disaster (as outlined in Table 3).

4 Results

4.1 Causal mechanism and evolution processes of MLG debris flow hazard chain

4.1.1 Rainstorm triggered the initiation of the hazard chain in MLG

Between 23:40 on 16 June 2020, and 02:30 on 17 June 2020, a heavy rainstorm impacted most townships in Danba County, with a particularly intense, short-term heavy rainfall episode occurring in the area of Banshanmen Township. Local interviews with villagers revealed that the debris flow in MLG began at approximately 3:00 p.m. on June 17. While the debris flow initiation was somewhat delayed compared to the onset of rainfall, it was generally consistent with the period of maximum rainfall intensity. According to the contour rainfall map found in the "Small and medium-sized watersheds in Sichuan Province rainstorm and flood calculation manual," the average 24-h maximum rainfall in the Banshanmen area of Danba County is typically around 40 mm. In the mountainous regions of Sichuan, debris flows are often triggered by rainfall amounts of approximately 48–50 mm for a single rainfall event (or 8–12.2 mm for a 10-min rainfall, or 0.8–1.2 mm for a 1-min rainfall). On June 17, the cumulative rainfall in Danba County reached only 16.2 mm (Figure 4). However, data from the county reported a 24-h rainfall of 59.9 mm in the mountainous area of Bawang Township, situated on the rear side of MLG, at 2:00 a.m.

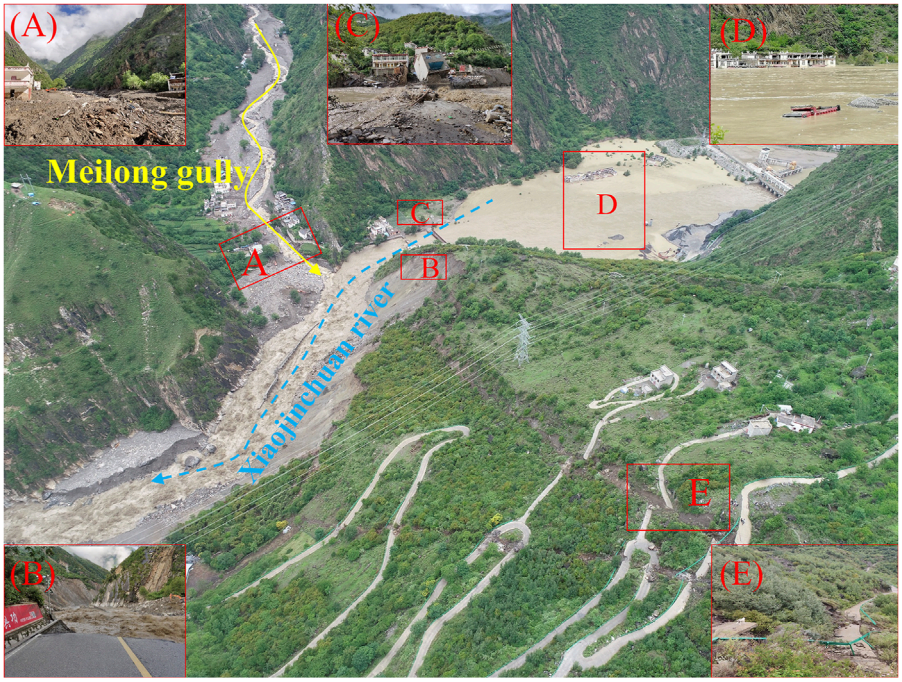

FIGURE 3
MLG debris flow hazard chain. **(A)** MLG debris flow destroyed and buried the houses in the gully mouth **(B)** MLG debris flow destroyed the national highway G350 and The debris flow destroyed the national highway G350 and triggered the resurrection of ANZ landslide on the opposite bank. **(C)** Outburst flood destroyed houses along the coast. **(D)** Barrier lake inundated houses and vehicles. **(E)** Cracks at the back end of landslide ANZ landslide.

on June 17. Based on established rainfall criteria, this amount classifies as a heavy rainstorm. Therefore, it can be inferred that the immediate trigger of the hazard chain was the short-term intense rainfall (Fiorillo and Wilson, 2004; Chen et al., 2006; Ni et al., 2014; Guo et al., 2016).

4.1.2 Earthquakes, landforms, and lithology provided abundant source of materials for the initiation of the hazard chain

The distinctive geomorphology and tectonics of the study area form a favorable foundation for the development of the MLG hazard chain. Situated within a typical alpine canyon landscape, this region lies at the structural heart of the Qinghai-Tibet-Yunnan-Burma-Indonesia tectonic complex. It encompasses north-south trending structures prevalent in the Sichuan-Yunnan region and arc-shaped structures in the Xiaojin-Jintang composite area. The study area is adjacent to the Xianshuihe fault belt, characterized by intense tectonic activity and the development of structural fractures, resulting in frequent regional seismic events. Extensive research has demonstrated that the aftermath of earthquakes significantly amplifies the availability of loose material sources in affected regions (Fan et al., 2019). Earthquakes disrupt the original integrity of rock and soil structures, thereby facilitating the transition of weathered surface rock masses into potential debris flow sources (Keefer, 1984). Moreover, they lower the rainfall threshold required to initiate instability in these material sources. The study area has witnessed several strong earthquakes in its history, with seven earthquakes identified as having significant impacts on soil stability, based on earthquake data acquired from the China Earthquake Data Center (http://data.earthquake.cn) from 1 January 1970, to 17 June 2020. Notably, the most recent three seismic events, including the 8.0 magnitude Wenchuan earthquake in 2008, the

TABLE 2 Calculation table of debris flow density.

Sample	Weight (kg)	Volume (m^3)	Density (g/cm^3)
PJ1	13.04	7.5	1.739
PJ2	14.92	8.46	1.764
PJ3	15.2	8.6	1.767
PJ4	11.13	6.25	1.781
PJ5	13.22	7.32	1.806
PJ6	12.5	6.95	1.799
PJ7	14.23	7.85	1.813
PJ8	14.82	8.25	1.796
PJ9	14.51	8.15	1.780
PJ10	14.35	8.35	1.719
PJ11	14.23	8.1	1.757
PJ12	14.51	8.5	1.707

TABLE 3 Calculation of debris flow velocity and discharge of different cross-sections.

Position	Mud depth H_c (m)	Channel gradient I_c	Roughness coefficient 1/n	Velocity V_c (m/s)	Area (m^2)	Discharge (m^3/s)
S1	4.50	0.229	3.7	4.88	99.00	483.12
S2	12.80	0.220	2.5	6.35	153.60	975.36
S3	5.20	0.214	3.7	5.53	208.00	1150.24
S4	4.80	0.213	3.7	5.62	168.00	944.16
S5	4.60	0.212	3.7	5.45	161.00	877.45
S6	4.55	0.213	3.7	4.78	180.00	860.40

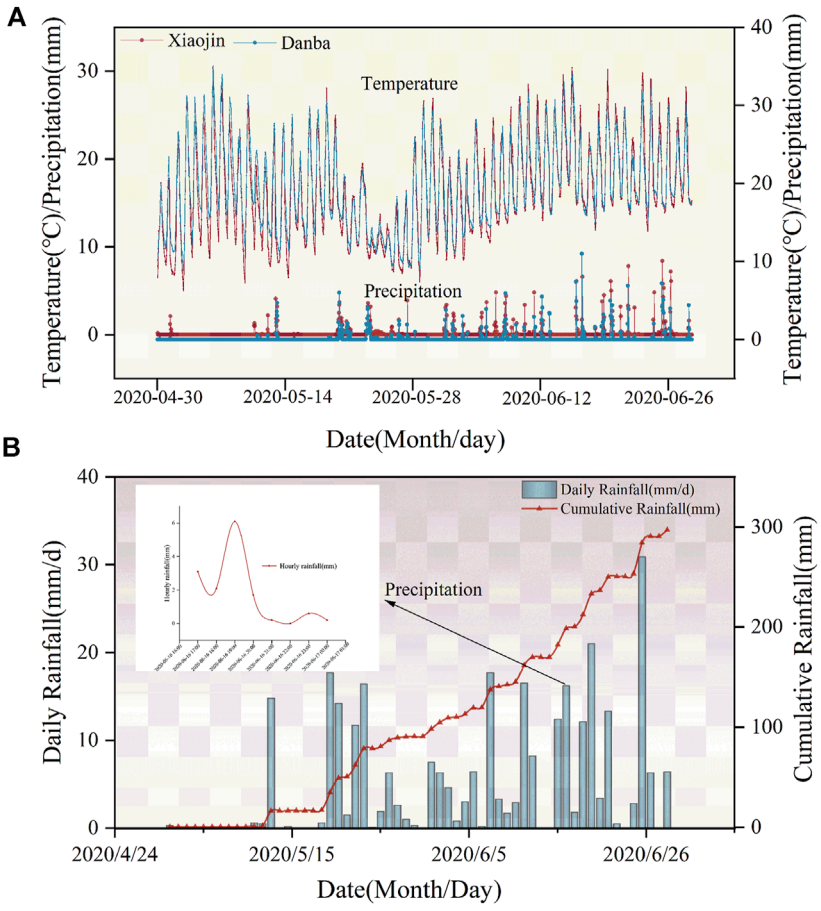

FIGURE 4
Daily rainfall data of two adjacent rainfall stations nearby **(A)** Daily rainfall at Xiaojin and Danba Station **(B)** Daily rainfall at MLG.

7.0 magnitude Lushan earthquake in 2013, and the 6.3 magnitude Kangding earthquake in 2014, all had substantial effects on material source stability within the watershed. These earthquakes have provided the necessary material sources for debris flows and subsequent hazard chains (Figure 5). Past research (Ding et al., 2020; Wang et al., 2022a; Liu et al., 2022; Yan et al., 2023) has indicated that in major tectonic zones, debris flows often concentrate in areas containing metamorphic rock formations like slate, phyllite, gneiss, mixed granite, and quartzite, along with softer rock formations such as mudstone, shale, marl, coal-bearing series, and Quaternary deposits. According to geological maps and field investigations, the exposed strata in the study area predominantly comprise granitic metamorphic rocks, slate, and phyllite from the Weiguan Group of the Devonian System (Dwg), in addition to lose deposits from

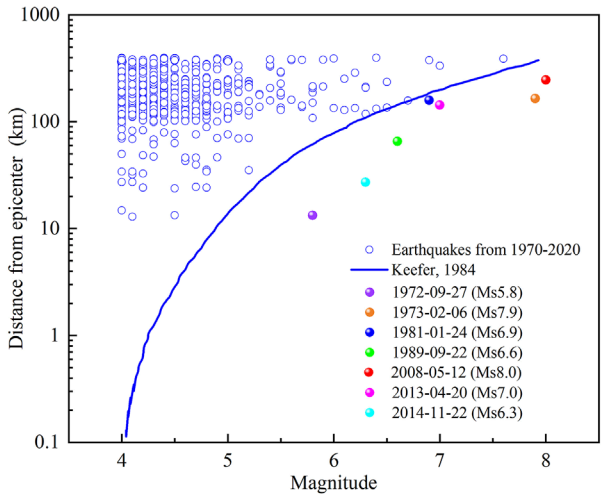

FIGURE 5
Historical earthquake impact map around the MLG.

the Quaternary System. These geological characteristics, coupled with the impact of earthquakes, establish a solid foundation for the initiation of the hazard chain.

Field investigations show that loose solid material sources are very abundant in the MLG watershed, and the main types of material sources in MLG are landslide-type material sources, channel accumulation-type material sources, slope-type material sources and freeze-thaw-type material sources (Figure 6). A total of 212 material sources points were investigated in the study area. Preliminary statistics reveal that there are 112 landslide accumulation solid material source points in the watershed, with a total volume of 7709.73×10^4 m^3 and a potential dynamic storage volume of 1285.48×10^4 m^3 that may contribute to debris flow activities. There are 28 channel accumulation solid material source points, with a total volume of 503.14×10^4 m^3 and a dynamic storage volume of 175.68×10^4 m^3. Additionally, there are 48 slope erosion solid material source points, with a total volume of 101.11×10^4 m^3 and a dynamic storage volume of 10.45×10^4 m^3. There are 22 freeze-thaw material source points, with a total volume of 1731.17×10^4 m^3 and a dynamic storage volume of 141.72×10^4 m^3. Furthermore, there are 2 artificial waste slag disposal points, with a total volume of 0.71×10^4 m^3 and a dynamic storage volume of 0.19×10^4 m^3. In total, the loose solid material sources amount to 10045.86×10^4 m^3, with a potential dynamic storage volume of 1613.52×10^4 m^3 that may contribute to debris flow activities (Table 4).

The material sources found in the MLG watershed exhibit distinct characteristics and distribution patterns, each playing a role in debris flow dynamics under the influence of heavy rainfall and floods. Landslide accumulation material sources are concentrated points of distribution and actively participate in debris flow movement as they are scoured and entrained by heavy rainfall and floods. Channel material sources primarily originate from the accumulation of the original channel, often evolving from landslide material sources and slope erosion material sources. Slope erosion material sources are predominantly located in the surface residual slope deposits on both sides of various tributaries and primarily contribute to debris flow activities through soil erosion. Freeze-thaw material sources, on the other hand, are typically situated near the snowline, representing frozen and thawed collapse material sources located on the thin ridges adjacent to the snowline. The abundance of loose solid materials in the MLG watershed is of paramount importance in understanding the occurrence of large-scale, low-frequency debris flow events, aligning with findings from prior research in this field (Bovis and Jakob, 1999; McGuire et al., 2017).

4.1.3 Multiple cycles of dry-wet cycle in the early stages facilitated the occurrence of the hazard chain in MLG

Multiple dry-wet cycle events in the early stages provided the triggering material source for the outbreak of the MLG debris flow in the hazard chain, promoting the occurrence of the hazard chain. The Standardized Precipitation Index (SPI) can be used to assess drought characteristics and determine the cycle of drought events (Schneider et al., 2013; Keyantash, 2021; Pei et al., 2023). The 1-month SPI results obtained from the analysis of the long-duration rainfall in the study area over a period of 70 years, from 1950 to 2020 (Figure 7), it indicates that at least 27 dry-wet cycle events occurred in MLG watershed prior to the outbreak of the debris flow. Among these 27 dry-wet cycle events, there were 6 moderately dry-moderately wet events, 8 extremely dry-moderately wet events, 1 extremely dry-severely wet event, 8 severely dry-moderately wet events, 3 moderately dry-extremely wet events and 1 severely dry-extremely wet event. A severe drought with an SPI value of −1.69 occurred in March 2020, the year of the MLG debris flow. Subsequently, a short but intense rainfall event on 17 June 2020 triggered the formation of the MLG debris flow. Dry-wet cycle events cause cracking of the soil surface, enhanced physical weathering, and reduced soil strength by altering the structure of the soil mass (Chiarle et al., 2007; Wei et al., 2010; Chen et al., 2014; Yang et al., 2023a), thus making it more susceptible to damage under heavy rainfall conditions. Therefore, the preceding occurrence of 27 moderate or higher intensity dry-wet cycle events significantly facilitated the outbreak of large-scale debris flow in MLG by reducing the strength of the soil mass and increasing the number of potential triggering material sources.

4.1.4 The cascading failure of large-scale landslides and channel-blocking boulders amplified the scale of the hazard chain

In order to analyze the evolution process of the MLG debris flow discharge, six cross-sections were selected (Tables 2, 3) within the MLG watershed, and the density, velocity, and discharge of the debris flow at each cross-section were calculated. Additionally, based on remote sensing images and field investigation, three major landslide dam breach points were identified within the MLG channel, namely, the Dongfengpengzi (DFPZ) landslide, Danyi village (DYV) landslide, and Meilong village (MLV) landslide (Figure 1). The discharge of the debris flow after the breach of these three dam points were as follows: No. 1 discharge was 483.12 m^3/s, No. 2 discharge was 975.36 m^3/s and No. 3 discharge was 1150.24 m^3/s (Figure 8). These three landslide dam breach points represent a sharp increase in the debris flow discharge during the evolution process. DFPZ landslide is located on the left bank slope of the main channel of MLG, approximately 3.43 km away from the outlet. The channel at

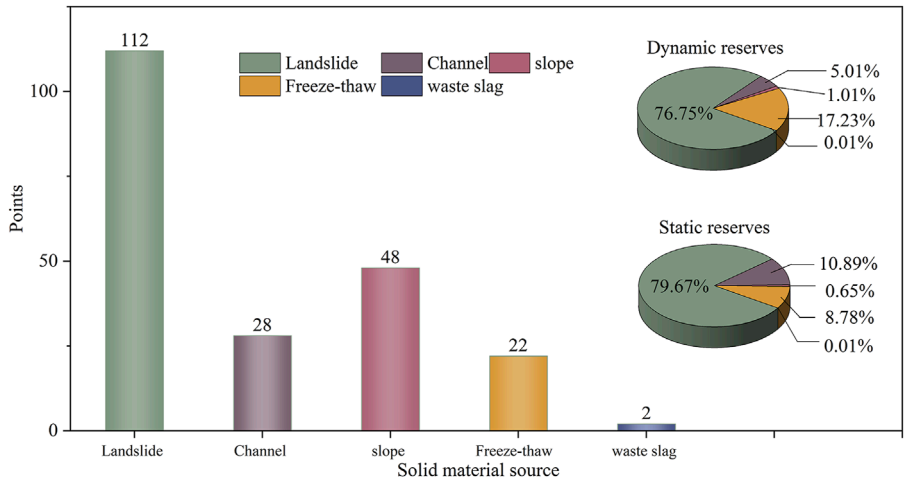

FIGURE 6
Typical material sources in MLG.

TABLE 4 Typical material sources statistics.

Solid material source	Points	Volume (10^4m^3)	Dynamic reserve (10^4m^3)
Landslide	112	7709.74	1285.48
Channel	28	503.14	175.68
slope	48	101.11	10.45
Freeze-thaw	22	1731.17	141.72
waste slag	2	0.71	0.19
Total	212	10045.86	1613.52

the foot of the slope is narrow, with a width of about 3 m–10 m, while its upstream channel has a width of about 40 m–80 m, with an average width of about 60 m. DYV landslide is situated on the right bank slope of the main channel of MLG, approximately 2.78 km away from the outlet. The channel at this location is narrow, with a width of about 3 m–9 m, and exhibits overall meandering with local blockages and clear traces of lateral erosion. MLV landslide is located on the right bank slope of the main channel of MLG, approximately 1.65 km away from the outlet. The channel at the foot of the slope is highly meandering, with a width of about 6 m–10 m, and boulders all over the ditch, and is scattered with boulders ranging from 3 m to 6 m in size. Its upstream channel is slightly wider, with an average width of about 15 m–20 m.

When the debris flow reaches the foot of the DFPZ landslide, the narrow channel and reduced cross-sectional area result in a rapid increase in flow velocity. The high-speed debris flow causes intense lateral erosion at the foot of the landslide. Additionally, continuous rainfall infiltration over a prolonged period weakens the stability of the DFPZ landslide. The intense lateral erosion leads to secondary sliding at the front edge of the landslide (Wang et al., 2022b; Ma et al., 2023), resulting in a blockage that accumulates loose material carried by the debris flow. Simultaneously, the increasing upstream water level and the accumulation of energy lead to the abrupt breaching of the landslide dam. As the debris flow moves towards the DYV landslide, the blockage effect further amplifies the flow velocity and discharge. This intensifies the erosion of the channel bed and banks, resulting in the unloading of the front edge of the DYV landslide to slide. Additionally, the direct impact of the debris flow at the channel diversion points lead to significant sliding at the front edge of the bank slope, causing a secondary blockage (Qiu et al., 2022). When the debris flow continues to move to the foot of MLV landslide, the narrowing of the channel results in a reduction in the cross-section, and an increase in flow velocity, enhancing the erosion process. Furthermore, the debris flow, which has already experienced the secondary blockage at DYV landslide, has its flow velocity and discharge multiplied several times, resulting in more intense erosion of the MLV landslide. This leads to extensive sliding at the front edge of the landslide, with a large number of debris and boulders occupying the channel, forming another blockage. The "6.17"MLG debris flow was significantly enhanced by the large-scale cascading blockage of the DFPZ landslide, DYV landslide, MLV landslide and the boulders in the channel, leading to a large amount of solid material being discharged at the outlet of the channel, triggering subsequent secondary hazard chains.

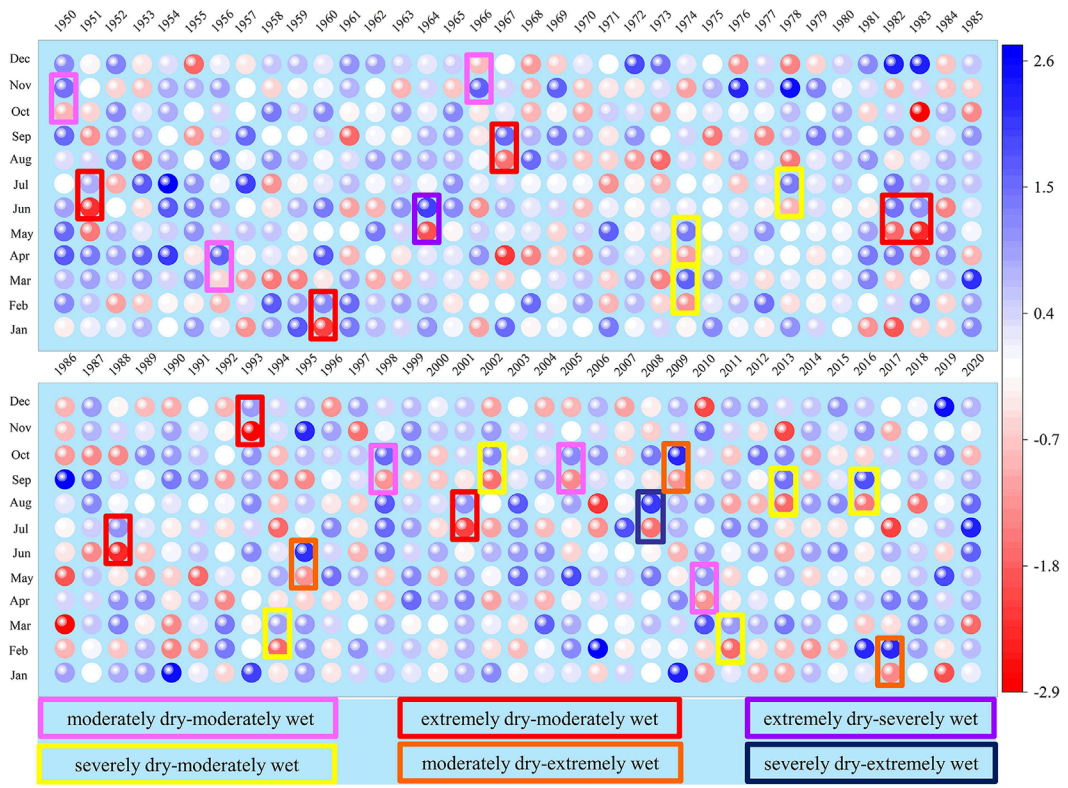

FIGURE 7
1-month SPI values in the study area over the period 1950-2020(Interpretation: SPI≥2, extremely wet; 1.5<SPI≤1.99, severely wet; 1.0<SPI≤1.49, moderately wet; −0.99<SPI≤0.99, near normal; −1.49<SPI≤−1.0, moderately dry; −1.99<SPI≤−1.5, severely dry; SPI≤−2, extremely dry).

4.2 Mitigation measures analysis of chain-breaking

The hazard chain is generally classified into four sections: the hazard pregnancy ring, the triggering ring, the evolution ring, and the damage ring. In the MLG watershed, lithology, geomorphology, pre-seismic activity and dry-wet cycle impacts provide the material and energy basis for the occurrence of the hazard chain, constituting the hazard pregnancy ring. Heavy rainfall as the triggering factor, representing the triggering ring. The amplification process of debris flows and the deformation process of landslides constitute the evolution. The resulting debris flows, landslides, barrier lakes and outburst floods form the damage ring.

Chain breaking refers to interrupting the development of the hazard chain at a certain link of the chain. For the MLG hazard chain, different chain breaking measures should be implemented in different rings (Figure 9). The MLG hazard chain is initiated by heavy rainfall, and the hazardous area is large in scope. It poses a major threat to the reconstructed National Highway G350 and vehicle operations through debris flow impact, siltation, and flood submergence, etc. and at the same time, threatens the lives and property of 99 individuals in 18 households at the gully mouth. So, breaking the hazard chain is necessary. Due to the huge amount of material sources in the MLG watershed, it is impractical to completely remove all debris flow sources. Therefore, engineering measures can be taken at the damage ring, such as constructing sediment retaining dams within debris flow channel, and establishing debris flow drainage canal at the gully mouth. Based on the sediment transport capacity of the XJC River segment, it is recommended to limit the debris flow discharge into the river to within 50,000 cubic meters per event to ensure the flood control and sediment transport capacity of the XJC River.

5 Discussion

The formation and amplification process MLG hazard chain are dominated by the material sources, and the increase in the amount of material sources can be influenced by strong regional tectonic activity and earthquakes (Figure 10). MLG watershed is located in the Sichuan-Yunnan north-south trending tectonic zone and the arc-shaped Xiaojin-Jintang tectonic zone, belonging to Tibetan-Yunnan-Burma-Indonesian tectonics. The tectonic system in the area is complex, with intense metamorphism, which favors the transformation of weathered surface rock masses into debris flow and landslide material sources. In addition, the study area and its neighboring regions experience frequent seismic activities, with multiple strong earthquakes have occurred in history. The latest strong earthquake to the time before the debris flow occurred was the 8.0 magnitude mega-earthquake that occurred on 12 May 2008 in Yingxiu Town, Wenchuan County. This earthquake had a

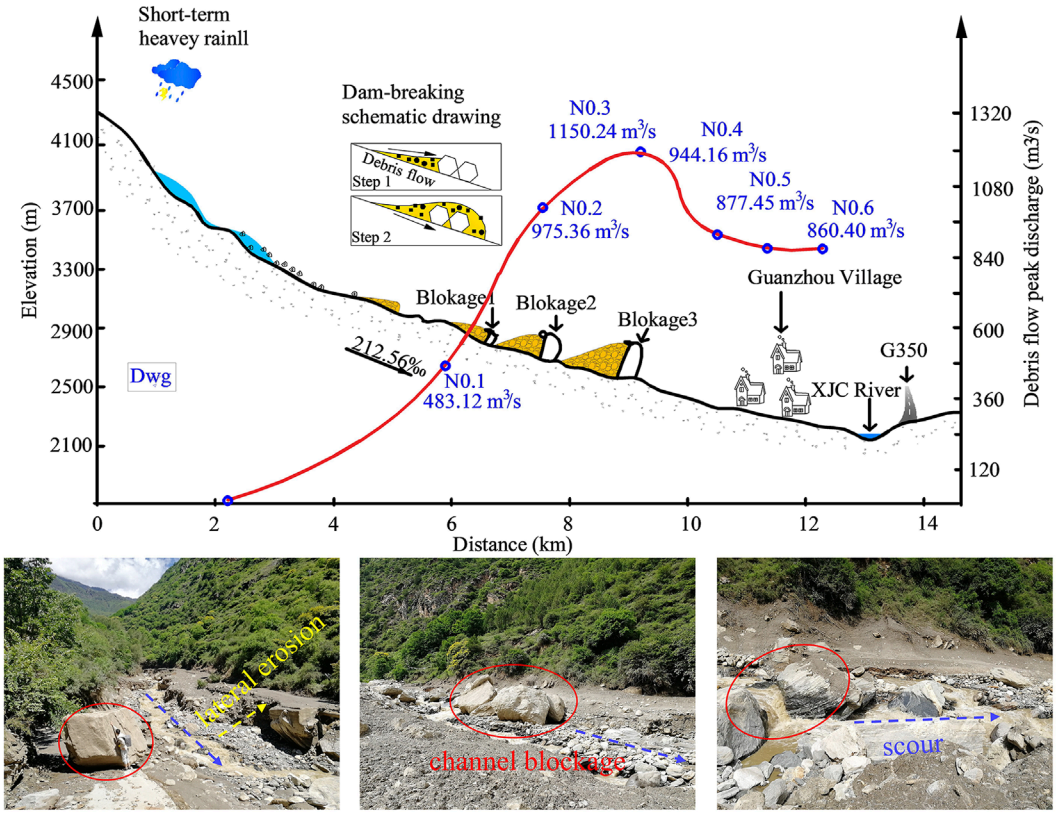

FIGURE 8
The discharge evolution process and photos of blockages of MLG debris flow.

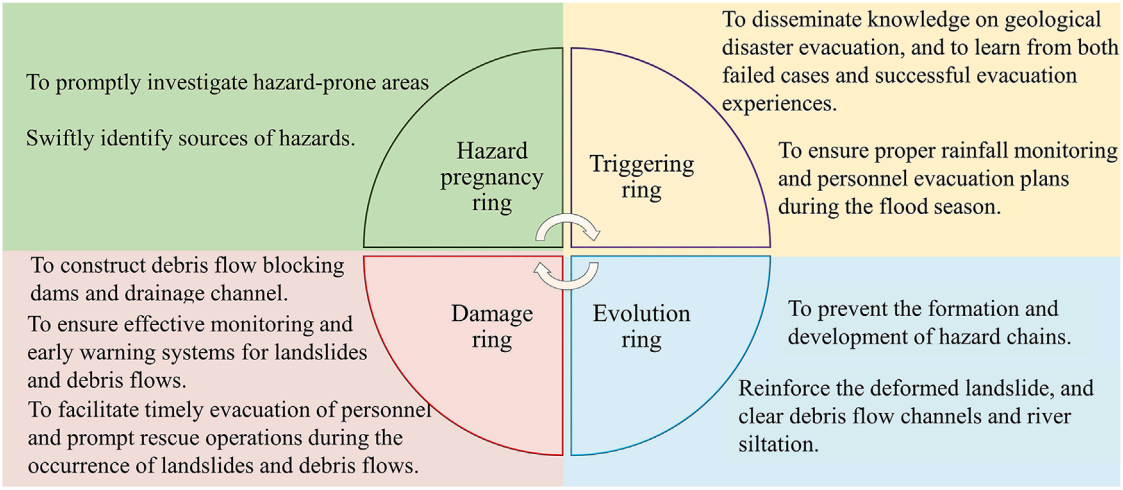

FIGURE 9
Suggestions on chain breaking measures in each link of hazard chain.

certain impact on the formation of material sources in the watershed, as an 8.0 magnitude earthquake can affect landslides up to a distance of 393 km (Delgado et al., 2011), while the study area is approximately 300 km away from the epicenter of the Wenchuan earthquake. Furthermore, previous research has indicated that the 2008 Wenchuan earthquake generated between 5 and 15 billion cubic meters of loose solid material within an area of 13,800 km^2 (Parker et al., 2011).

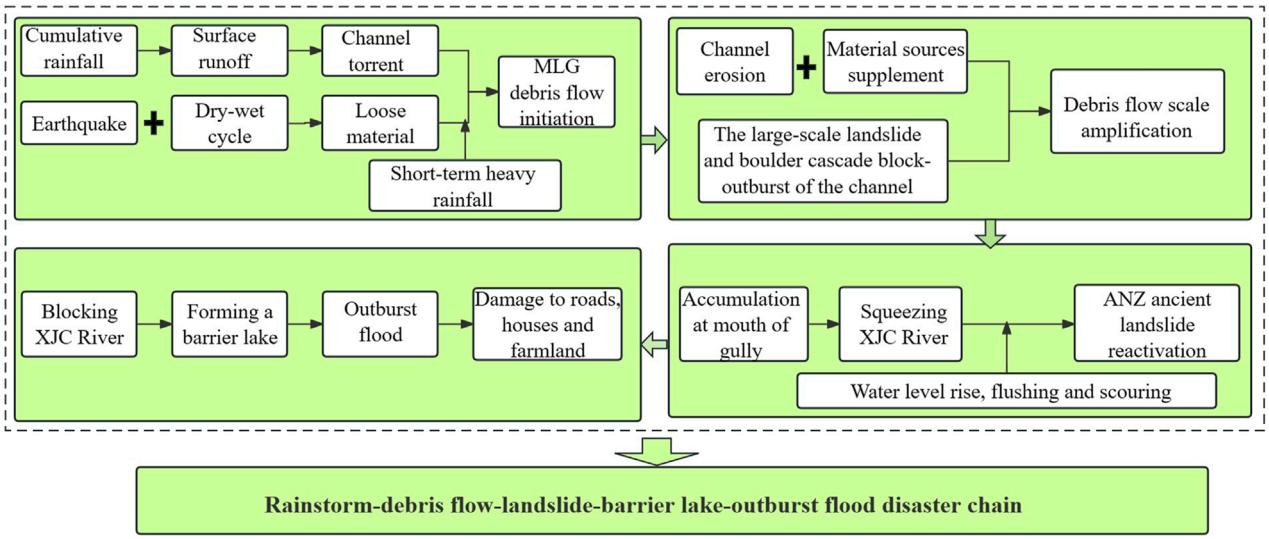

FIGURE 10
The whole process of MLG debris flow hazard chain.

Currently, the amount of loose solid material sources in the MLG watershed that may be involved in debris flow activities are estimated to be 1613.52×10^4 m^3. These sources are distributed in the main channel and various tributaries, but they do not all participate in debris flow activity simultaneously. Furthermore, not all loose solid material sources involved in a single debris flow activity event will be completely washed out of the debris flow channel and enter into the main river. First of all, the MLG watershed has a large area, and rainfall distribution cannot be completely uniform. There may be areas within the watershed where loose solid materials are present but do not meet the conditions for rainfall initiation or there may be no distribution of loose solid materials in areas of heavy rainfall. This rainfall distribution of the unevenness also determines the uneven participation of loose solid materials in debris flow activity. Secondly, not all loose solid materials in tributary channels can participate in debris flow activity in the main channel. With changes in channel slope and width, water-sediment separation can occur in certain sections, resulting in sediment accumulation in the channel. Therefore, the transformation of debris flow sources is a complex process (Yang et al., 2023c; Zhao et al., 2023), and the design of prevention and control engineering is mainly based on the historical records of debris flow disasters and the calculation results of previous debris flow characteristics.

In addition, the on-site investigation has revealed that the sliding of the avalanche deposits at the front edge of the ANZ landslide drove the collapse of the strongly weathered bedrock to form the accumulation at the foot of slope, creating the illusion of bedrock sliding. Salt efflorescence refers to the phenomenon where underground water containing soluble salts flows to the surface and, due to the decrease in atmospheric pressure and increase in temperature, the minerals precipitate and crystallize. Previous studies have shown that the shear strength of the soil decreases continuously after the precipitation of soluble salts, leading to slow deformation of the slope. The cyclic process of leaching and precipitation of soluble salts in groundwater ultimately results in the instability or reactivation of landslides (Zhang et al., 2020b). The boundary between the landslide deposits and the highly weathered bedrock in ANZ landslide is marked by the presence of salt efflorescence. Therefore, it can be inferred that this boundary represents the discharge point of the previous groundwater, and the lower part of the landslide deposit serves as the shear outlet of the landslide. The identification of the salt efflorescence outcrops can help to determine whether the ANZ landslide is characterized by local surface sliding or overall sliding, which is a guide for determining the morphologic characteristics of the blocked barrier dam and the formulation of hazard prevention and mitigation measures. Additionally, it provides new insights and references for understanding the mechanisms of landslide formation, identifying slope instability and the reactivation of paleolandslides in mountainous urban areas.

The MLG hazard chain and the formation of material sources for debris flows and landslides share similarities with other regions around the world that have experienced strong tectonic activity and earthquakes. For example, the 2011 Tohoku earthquake in Japan triggered numerous landslides and debris flows, leading to significant damage and loss of life (Mukunoki et al., 2016). In 2018, the Sulawesi earthquake in Indonesia triggered landslides that buried entire villages, causing widespread devastation (Watkinson and Hall, 2019; Zhao, 2021). In both cases, the formation of material sources for debris flows and landslides was influenced by the seismic activity. The impact of rainfall distribution on the participation of loose solid materials in debris flow activity is also a common factor in other regions. For instance, in the Himalayan region, the uneven distribution of rainfall and the presence of loose solid materials in steep slopes have led to frequent landslides and debris flows (Burtin et al., 2009; Das et al., 2022). In the Andes

Mountains, the combination of steep topography, intense rainfall, and the presence of loose sediments has resulted in frequent debris flows and landslides (Moreiras and Dal Pont, 2017; Angillieri et al., 2020). The role of salt efflorescence in influencing the stability of slopes and the cyclic process of leaching and precipitation of soluble salts leading to slow deformation is also a mechanism that may have relevance in other regions with similar geological and topographical characteristics. For example, in the Ebro Valley (NE Spain), the presence of salt efflorescence on slopes has been linked to the destabilization of slopes and the occurrence of landslides (Gutiérrez et al., 2023).

In conclusion, the MLG hazard chain and the mechanisms of debris flow and landslide formation share similarities with other regions around the world that have experienced strong tectonic activity, earthquakes, and intense rainfall. Studying international cases with similar geological and environmental characteristics could provide valuable insights for understanding and managing hazards related to debris flows, landslides, and slope instability in various parts of the world.

6 Conclusion

In order to investigate the triggering mechanism of landslide-debris flow hazard chain in mountainous urban areas, this study focuses on the hazard chain of MLG debris flow-ANZ landslide-barrier lake -outburst flood that occurred in Danba County, Sichuan Province, on 17 June 2020. Through on-site investigations, model calculations, rainfall analysis, seismic impact analysis, and drought index analysis, the characteristic parameters of the MLG hazard chain were obtained, the hazard pregnancy factors were analyzed, the triggering mechanism of the MLG hazard chain was revealed, and measures to break the hazard chain at different links were proposed. It is helpful to improve the early warning and forecasting system of urban monitoring in western Sichuan mountainous area and grasp the key direction of engineering prevention and control. The conclusions of our research are as follows:

(1) The low-frequency large-scale debris flow disaster in MLG, which occurred on 17 June 2020, has a recurrence interval of approximately 70 years, with an average density of 1.769 g/cm^3. The flow velocity of the debris flow at the outlet of the gully is 4.78 m/s, and the peak flow discharge is 860.40 m^3/s. The tremendous energy of the debris flow forms the basis for the destructive power of the hazard chain.

(2) The unique geomorphology and lithology of the study area provide favorable conditions for the occurrence of the hazard chain in MLG. Seven seismic events, including the Wenchuan 8.0 magnitude earthquake in 2008, have had a significant impact on the stability of the soil mass in the MLG watershed. The occurrence of the large-scale debris flow in MLG was facilitated by the occurrence of 27 moderate and above dry-wet cycle events in the previous period, which reduced the soil strength and increased the availability of material sources. Under the influence of internal and external dynamic forces such as earthquakes, drought, and rainfall, the structure of geotechnical bodies in the MLG watershed was continuously damaged, which accelerated the weathering and erosion of the geotechnical bodies and led to a significant increase in the amount of loose material sources in the watershed. The abundant loose solid material sources in the MLG watershed are the key factors contributing to the outbreak of this large-scale low-frequency debris flow.

(3) The MLG hazard chain is characterized by the presence of three large landslides, namely, DFPZ landslide, DYV landslide, and MLV Village landslide, along with the cascading blockage and breach caused by giant boulders within the channel. This has resulted in a 2.38-fold increase in the debris flow discharge within the 1.78 km-long channel, significantly enhanced the energy of the debris flow and leading to the ejection of a large amount of solid material from the outlet, triggering subsequent secondary disaster chains.

(4) The rainstorm-induced hazard chain in MLG is a complete composite geological hazard chain, forming a hazard chain of rainstorm, debris flow, landslide, barrier lake and outburst flood. For the hazard chain of MLG, chain-breaking measures are proposed at different links. It is recommended to take chain-breaking measures from the damage ring, strengthen the monitoring and early warning during flood season, and construct debris flow blocking dams and drainage canals.

While the specifics of hazard chains may vary across different geographic locations, the principles of hazard chain analysis and the importance of implementing chain-breaking measures are universally applicable. Therefore, our study also provides insights into the triggering mechanisms and characteristics of the MLG hazard chain, offering valuable lessons for similar hazard chains in other regions worldwide. Our findings contribute to the broader understanding of hazard chain dynamics and can inform disaster risk reduction strategies in other settings. The information about the casualties and destruction caused by the hazard chain serves as a reminder of the devastating impact of such disasters and underscores the urgency of proactive measures to mitigate their effects.

Data availability statement

The original contributions presented in the study are included in the article/Supplementary material, further inquiries can be directed to the corresponding author.

Author contributions

HS: Conceptualization, Investigation, Methodology, Software, Writing–original draft, Writing–review and editing. ZY: Conceptualization, Funding acquisition, Project administration, Supervision, Writing–original draft. GH: Investigation, Writing–review and editing. ST: Investigation, Writing–review and editing. MR: Writing–review and editing. JR: Data curation,

Investigation, Writing–original draft. YZ: Data curation, Investigation, Writing–review and editing.

Funding

The author(s) declare financial support was received for the research, authorship, and/or publication of this article. This study was funded by the National Natural Science Foundation of China (Grant No. 41861134008), the Muhammad Asif Khan academician workstation of Yunnan Province (Grant No. 202105AF150076), the Key R&D Program of Yunnan Province (Grant No. 202003AC100002), the General Program of basic research plan of Yunnan Province (Grant No. 202001AT070043). Youth Science Foundation of Henan Province (No. 232300420449).

Conflict of interest

The authors declare that the research was conducted in the absence of any commercial or financial relationships that could be construed as a potential conflict of interest.

Publisher's note

References

An, H. C., Ouyang, C. J., Wang, F. L., Xu, Q. S., Wang, D. P., Yang, W. B., et al. (2022). Comprehensive analysis and numerical simulation of a large debris flow in the Meilong catchment, China. *Eng. Geol.* 298, 106546. doi:10.1016/j.enggeo.2022.106546

Angillieri, M. Y. E., Perucca, L., and Vargas, N. (2020). Spatial and temporal analysis of debris flow occurrence in three adjacent basins of the western margin of Grande River: quebrada de Humahuaca, Jujuy, Argentina. *Geogr. Ann. Ser. a-Physical Geogr.* 102 (2), 83–103. doi:10.1080/04353676.2020.1744075

Bovis, M. J., and Jakob, M. (1999). The role of debris supply conditions in predicting debris flow activity. *Earth Surf. Process. Landforms* 24 (11), 1039–1054. doi:10.1002/(sici)1096-9837(199910)24:11<1039::Aid-esp29>3.0.Co;2-u

Burtin, A., Bollinger, L., Cattin, R., Vergne, J., and Nábelek, J. L. (2009). Spatiotemporal sequence of Himalayan debris flow from analysis of high-frequency seismic noise. *J. Geophys. Research-Earth Surf.* 114, 15. doi:10.1029/2008jf001198

Chen, H., Dadson, S., and Chi, Y. G. (2006). Recent rainfall-induced landslides and debris flow in northern Taiwan. *Geomorphology* 77 (1-2), 112–125. doi:10.1016/j.geomorph.2006.01.002

Chen, N. S., Lu, Y., Zhou, H. B., Deng, M. F., and Han, D. W. (2014). Combined impacts of antecedent earthquakes and droughts on disastrous debris flows. *J. Mt. Sci.* 11 (6), 1507–1520. doi:10.1007/s11629-014-3080-7

Chen, X. Q., Cui, P., Li, Y., and Zhao, W. Y. (2011). Emergency response to the Tangjiashan landslide-dammed lake resulting from the 2008 Wenchuan Earthquake, China. *Landslides* 8 (1), 91–98. doi:10.1007/s10346-010-0236-6

Chen, X.-z., and Cui, Y.-f. (2017). The formation of the Wulipo landslide and the resulting debris flow in Dujiangyan City, China. *J. Mt. Sci.* 14 (6), 1100–1112. doi:10.1007/s11629-017-4392-1

Cheng, J. D., Su, R. R., and Wu, H. L. (2000). "Hydrometeorological and site factors contributing to disastrous debris-flows in Taiwan," in 2nd International Conference on Debris-Flow Hazards Mitigation, LEIDEN (A a Balkema Publishers), 583–592.

Chiarle, M., Iannotti, S., Mortara, G., and Deline, P. (2007). Recent debris flow occurrences associated with glaciers in the Alps. *Glob. Planet. Change* 56 (1-2), 123–136. doi:10.1016/j.gloplacha.2006.07.003

Cui, P., Su, F., Zou, Q., Chen, N., and Zhang, Y. (2015). Risk assessment and disaster reduction strategies for mountainous and meteorological hazards in Tibetan Plateau. *Chin. Sci. Bull.* 60 (32), 3067–3077. doi:10.1360/N972015-00849

Das, R., Phukon, P., and Singh, T. N. (2022). Understanding the cause and effect relationship of debris slides in Papum Pare district, Arunachal Himalaya, India. *Nat. Hazards* 110 (3), 1735–1760. doi:10.1007/s11069-021-05010-2

Deganutti, A. M., Marchi, L., and Arattano, M. (2000). "Rainfall and debris-flow occurrence in the Moscardo basin (Italian Alps)," in 2nd International Conference on Debris-Flow Hazards Mitigation, LEIDEN (A a Balkema Publishers), 67–72.

Delgado, J., Garrido, J., Lopez-Casado, C., Martino, S., and Pelaez, J. A. (2011). On far field occurrence of seismically induced landslides. *Eng. Geol.* 123 (3), 204–213. doi:10.1016/j.enggeo.2011.08.002

Ding, M., Huang, T., Zheng, H., and Yang, G. (2020). Respective influence of vertical mountain differentiation on debris flow occurrence in the Upper Min River, China. *Sci. Rep.* 10 (1), 11689. doi:10.1038/s41598-020-68590-2

Fan, X., Domènech, G., Scaringi, G., Huang, R., Xu, Q., Hales, T. C., et al. (2018). Spatio-temporal evolution of mass wasting after the 2008 Mw 7.9 Wenchuan earthquake revealed by a detailed multi-temporal inventory. *Landslides* 15 (12), 2325–2341. doi:10.1007/s10346-018-1054-5

Fan, X. M., Scaringi, G., Korup, O., West, A. J., van Westen, C. J., Tanyas, H., et al. (2019). Earthquake-induced chains of geologic hazards: patterns, mechanisms, and impacts. *Rev. Geophys.* 57 (2), 421–503. doi:10.1029/2018rg000626

Fiorillo, F., and Wilson, R. C. (2004). Rainfall induced debris flows in pyroclastic deposits, Campania (southern Italy). *Eng. Geol.* 75 (3-4), 263–289. doi:10.1016/j.enggeo.2004.06.014

Flentje, P. N., Chowdhury, R. N., and Tobin, P. (2000). "Management of landslides triggered by a major storm event in Wollongong, Australia," in 2nd International Conference on Debris-Flow Hazards Mitigation, LEIDEN (A a Balkema Publishers), 479–487.

Guo, J., Cui, P., Qin, M., Wang, J., Li, Y., and Wang, C. (2022). Response of ancient landslide stability to a debris flow: a multi-hazard chain in China. *Bull. Eng. Geol. Environ.* 81 (7), 273. doi:10.1007/s10064-022-02745-5

Guo, J., Wang, J., Li, Y., and Yi, S. (2021). Discussions on the transformation conditions of Wangcang landslide-induced debris flow. *Landslides* 18 (5), 1833–1843. doi:10.1007/s10346-021-01650-4

Guo, X., Cui, P., Li, Y., Ma, L., Ge, Y., and Mahoney, W. B. (2016). Intensity–duration threshold of rainfall-triggered debris flows in the Wenchuan Earthquake affected area, China. *Geomorphology* 253, 208–216. doi:10.1016/j.geomorph.2015.10.009

Gutiérrez, F., Sevil, J., and Migon, P. (2023). Landslides in the Remolinos gypsum escarpment (NE Spain): controls imposed by stratigraphy, fluvial erosion, and interstratal salt dissolution. *Landslides* 20 (10), 2075–2093. doi:10.1007/s10346-023-02090-y

Guttman, N. B. (1999). Accepting the standardized precipitation index: a calculation algorithm. *J. Am. Water Resour. Assoc.* 35 (2), 311–322. doi:10.1111/j.1752-1688.1999.tb03592.x

Hu, G. S., Huang, H., Chen, N. S., Somos-Valenzuela, M., Yang, Z. Q., and He, J. (2022). Largest scale successful real-time evacuation after the Wenchuan earthquake in China: lessons learned from the Zengda gully giant debris flow disaster. *Geomatics Nat. Hazards Risk* 13 (1), 19–34. doi:10.1080/19475705.2021.2000045

Hu, K., Zhang, X., You, Y., Hu, X., Liu, W., and Li, Y. (2019). Landslides and dammed lakes triggered by the 2017 Ms6.9 Milin earthquake in the Tsangpo gorge. *Landslides* 16 (5), 993–1001. doi:10.1007/s10346-019-01168-w

Iotti, A., and Simoni, A. (1997). "A debris flow triggered by a soil slip on Elba Island, Italy," in 1st International Conference on Debris-Flow Hazards Mitigation - Mechanics, Prediction, and Assessment, NEW YORK (Amer Soc Civil Engineers), 54–63.

Keefer, D. K. (1984). LANDSLIDES CAUSED BY EARTHQUAKES. *Geol. Soc. Am. Bull.* 95 (4), 406–421. doi:10.1130/0016-7606(1984)95<406:Lcbe>2.0.Co;2

Keyantash, J. (2021). "Indices for meteorological and hydrological drought," in *Hydrological aspects of climate change*. Editors A. Pandey, S. Kumar, and A. Kumar (Singapore: Springer Singapore), 215–235.

Liu, D., Cui, Y., Jin, W., Wang, H., and Tang, H. (2023a). Channel aggradation triggered by dam failure amplifies the damage of outburst flood. *Landslides* 20 (7), 1343–1362. doi:10.1007/s10346-023-02026-6

Liu, Z. J., Qiu, H. J., Zhu, Y. R., Liu, Y., Yang, D. D., Ma, S. Y., et al. (2022). Efficient identification and monitoring of landslides by time-series InSAR combining single- and multi-look phases. *Remote Sens.* 14 (4), 1026. doi:10.3390/rs14041026

Liu, Z. Q., Yang, Z. Q., Chen, M., Xu, H. H., Yang, Y., Zhang, J., et al. (2023b). Research hotspots and Frontiers of mountain flood disaster: bibliometric and visual analysis. *Water* 15 (4), 673. doi:10.3390/w15040673

Ma, S. Y., Qiu, H. J., Zhu, Y. R., Yang, D. D., Tang, B. Z., Wang, D. Z., et al. (2023). Topographic changes, surface deformation and movement process before, during and after a rotational landslide. *Remote Sens.* 15 (3), 662. doi:10.3390/rs15030662

Mani, P., Allen, S., Evans, S. G., Kargel, J. S., Mergili, M., Petrakov, D., et al. (2023). Geomorphic process chains in high-mountain regions-A review and classification approach for natural hazards assessment. *Rev. Geophys.* 61 (4), 51. doi:10.1029/2022rg000791

McGuire, L. A., Rengers, F. K., Kean, J. W., and Staley, D. M. (2017). Debris flow initiation by runoff in a recently burned basin: is grain-by-grain sediment bulking or en masse failure to blame? *Geophys. Res. Lett.* 44 (14), 7310–7319. doi:10.1002/2017gl074243

McKee, T. B., Doesken, N. J., Kleist, J., and Amer Meteorol, S. O. C. (1995). "Drought monitoring with multiple time scales," in 9th Conference on Applied Climatology/75th AMS Annual Meeting, BOSTON (Amer Meteorological Soc), 233–236.

Moreiras, S. M., and Dal Pont, I. P. V. (2017). "Climate change driving greater slope instability in the central Andes," in 4th World Landslide Forum (CHAM: Springer International Publishing Ag), 191–197.

Mukunoki, T., Kasama, K., Murakami, S., Ikemi, H., Ishikura, R., Fujikawa, T., et al. (2016). Reconnaissance report on geotechnical damage caused by an earthquake with JMA seismic intensity 7 twice in 28 h, Kumamoto, Japan. *Soils Found.* 56 (6), 947–964. doi:10.1016/j.sandf.2016.11.001

Ni, H. Y., Zheng, W. M., Song, Z., and Xu, W. (2014). Catastrophic debris flows triggered by a 4 July 2013 rainfall in Shimian, SW China: formation mechanism, disaster characteristics and the lessons learned. *Landslides* 11 (5), 909–921. doi:10.1007/s10346-014-0514-9

Ning, L., Hu, K., Wang, Z., Luo, H., Qin, H., Zhang, X., et al. (2022). Multi-hazard chain reaction initiated by the 2020 Meilong debris flow in the dadu river, southwest China. *Front. Earth Sci.* 10. doi:10.3389/feart.2022.827438

Parker, R. N., Densmore, A. L., Rosser, N. J., de Michele, M., Li, Y., Huang, R., et al. (2011). Mass wasting triggered by the 2008 Wenchuan earthquake is greater than orogenic growth. *Nat. Geosci.* 4 (7), 449–452. doi:10.1038/ngeo1154

Pei, Y. Q., Qiu, H. J., Yang, D. D., Liu, Z. J., Ma, S. Y., Li, J. Y., et al. (2023). Increasing landslide activity in the Taxkorgan River Basin (eastern Pamirs Plateau, China) driven by climate change. *Catena* 223, 106911. doi:10.1016/j.catena.2023.106911

Pérez, F. L. (2001). Matrix granulometry of catastrophic debris flows (December 1999) in central coastal Venezuela. *CATENA* 45 (3), 163–183. doi:10.1016/S0341-8162(01)00149-7

Qiu, H. J., Zhu, Y. R., Zhou, W. Q., Sun, H. S., He, J. Y., and Liu, Z. J. (2022). Influence of DEM resolution on landslide simulation performance based on the Scoops3D model. *Geomatics Nat. Hazards Risk* 13 (1), 1663–1681. doi:10.1080/19475705.2022.2097451

Rahman, M. A., and Konagai, K. (2017). Substantiation of debris flow velocity from super-elevation: a numerical approach. *Landslides* 14 (2), 633–647. doi:10.1007/s10346-016-0725-3

Schneider, D. P., Deser, C., Fasullo, J., and Trenberth, K. E. (2013). Climate data guide spurs discovery and understanding. *Eos, Trans. Am. Geophys. Union* 94 (13), 121–122. doi:10.1002/2013EO130001

Scott, K. M. (2000). "Precipitation-triggered debris-flow at Casita Volcano, Nicaragua: implications for mitigation strategies in volcanic and tectonically active steeplands," in 2nd International Conference on Debris-Flow Hazards Mitigation, LEIDEN (A a Balkema Publishers), 3–13.

Seiler, R. A., Hayes, M., and Bressan, L. (2002). Using the standardized precipitation index for flood risk monitoring. *Int. J. Climatol.* 22 (11), 1365–1376. doi:10.1002/joc.799

Wang, F., Fan, X., Yunus, A. P., Siva Subramanian, S., Alonso-Rodriguez, A., Dai, L., et al. (2019). Coseismic landslides triggered by the 2018 Hokkaido, Japan (Mw 6.6), earthquake: spatial distribution, controlling factors, and possible failure mechanism. *Landslides* 16 (8), 1551–1566. doi:10.1007/s10346-019-01187-7

Wang, J., Cui, Y. F., Choi, C. E., and Ng, C. W. W. (2018). "The effect of climate change on alpine mountain hazards chain: a case study in tianmo ravine, Tibet, China," in 8th International Congress on Environmental Geotechnics (ICEG) (SINGAPORE: Springer-Verlag Singapore Pte Ltd), 461–470.

Wang, L., Chang, M., Le, J., Xiang, L., and Ni, Z. (2022a). Two multi-temporal datasets to track debris flow after the 2008 Wenchuan earthquake. *Sci. Data* 9 (1), 525. doi:10.1038/s41597-022-01658-y

Wang, L. Y., Qiu, H. J., Zhou, W. Q., Zhu, Y. R., Liu, Z. J., Ma, S. Y., et al. (2022b). The post-failure spatiotemporal deformation of certain translational landslides may follow the pre-failure pattern. *Remote Sens.* 14 (10), 2333. doi:10.3390/rs14102333

Watkinson, I. M., and Hall, R. (2019). Impact of communal irrigation on the 2018 Palu earthquake-triggered landslides. *Nat. Geosci.* 12(11), 940–945. doi:10.1038/s41561-019-0448-x

Wei, W., Chen, L. D., Fu, B. J., and Chen, J. (2010). Water erosion response to rainfall and land use in different drought-level years in a loess hilly area of China. *Catena* 81 (1), 24–31. doi:10.1016/j.catena.2010.01.002

Yan, Y., Hu, S., Zhou, K., Jin, W., Ma, N., and Zeng, C. (2023). Hazard characteristics and causes of the "7.22" 2021 debris flow in Shenshuicao gully, Qilian Mountains, NW China. *Landslides* 20 (1), 111–125. doi:10.1007/s10346-022-01992-7

Yang, Z. Q., Chen, M., Zhang, J., Ding, P., He, N., and Yang, Y. (2023a). Effect of initial water content on soil failure mechanism of loess mudflow disasters. *Front. Ecol. Evol.* 11. doi:10.3389/fevo.2023.1141155

Yang, Z. Q., Wei, L., Liu, Y. Q., He, N., Zhang, J., and Xu, H. H. (2023b). Discussion on the relationship between debris flow provenance particle characteristics, gully slope, and debris flow types along the karakoram highway. *Sustainability* 15 (7), 5998. doi:10.3390/su15075998

Yang, Z. Q., Xiong, J. F., Zhao, X. G., Meng, X. R., Wang, S. B., Li, R., et al. (2023c). Column-hemispherical penetration grouting mechanism for Newtonian fluid considering the tortuosity of porous media. *Processes* 11 (6), 1737. doi:10.3390/pr11061737

Yang, Z. Q., Zhao, X. G., Chen, M., Zhang, J., Yang, Y., Chen, W. T., et al. (2023d). Characteristics, dynamic analyses and hazard assessment of debris flows in niumiangou valley of wenchuan county. *Appl. Sciences-Basel* 13 (2), 1161. doi:10.3390/app13021161

Zhang, L., Xiao, T., He, J., and Chen, C. (2019). Erosion-based analysis of breaching of Baige landslide dams on the Jinsha River, China, in 2018. *Landslides* 16 (10), 1965–1979. doi:10.1007/s10346-019-01247-y

Zhang, X., Xue, R., Wang, M., Yu, Z., Li, B., and Wang, B. (2020a). Field investigation and analysis on flood disasters due to Baige landslide dam break in Jinsha River. *Adv. Eng. Sci.* 52 (5), 89–100.

Zhang, Z. L., Zeng, R. Q., Meng, X. M., Zhang, Y., Zhao, S. F., Ma, J. H., et al. (2020b). Effect of soluble salt loss via spring water on irrigation-induced landslide deformation. *Water* 12 (10), 2889. doi:10.3390/w12102889

Zhao, B. (2021). Landslides triggered by the 2018 Mw 7.5 Palu supershear earthquake in Indonesia. *Eng. Geol.* 294, 106406. doi:10.1016/j.enggeo.2021.106406

Zhao, X. G., Yang, Z. Q., Meng, X. R., Wang, S. B., Li, R., Xu, H. H., et al. (2023). Study on mechanism and verification of columnar penetration grouting of time-varying Newtonian fluids. *Processes* 11 (4), 1151. doi:10.3390/pr11041151

Zhong, Q. M., Chen, S. S., Wang, L., and Shan, Y. B. (2020). Back analysis of breaching process of Baige landslide dam. *Landslides* 17 (7), 1681–1692. doi:10.1007/s10346-020-01398-3